ԵՐԵՎԱՆԻ ՊԵՏԱԿԱՆ ՀԱՄԱԼՍԱՐԱՆ

ՀԱՅԱՍՏԱՆԻ ՀԱՆՐԱՊԵՏՈՒԹՅԱՆ ԳԻՏՈՒԹՅՈՒՆՆԵՐԻ
ԱԶԳԱՅԻՆ ԱԿԱԴԵՄԻԱ

ԿԻՍԱՀԱՂՈՐԴՉԱՅԻՆ ՄԻԿՐՈ- ԵՎ ՆԱՆՈԷԼԵԿՏՐՈՆԻԿԱ

ՏԱՍՆԱՄԵԿԵՐՈՐԴ ՄԻՋԱԶԳԱՅԻՆ ԳԻՏԱԺՈՂՈՎԻ ՆՅՈՒԹԵՐ
ԵՐԵՎԱՆ, 23-25 ՀՈՒՆԻՍ

SEMICONDUCTOR MICRO- AND NANOELECTRONICS

PROCEEDINGS OF THE ELEVENTH INTERNATIONAL CONFERENCE
YEREVAN, ARMENIA, JUNE 23-25

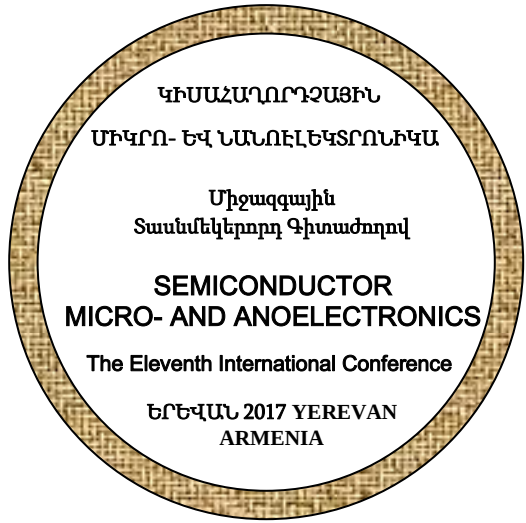

Երևան

ԵՊՀ հրատարակչություն

2017

BIOCHEMICAL SENSORS BASED ON SILICON NANORIBBON FETs
Part 2: Low-frequency noise and size-dependent effects

F. Gasparyan[1,2], I. Zadorozhnyi[2], H. Khondkaryan[1], A. Arakelyan[1], S. Vitusevich[2]

[1]*Yerevan State University, 1 Alex Manoogian St., 0025, Yerevan Armenia*
[2]*Peter Grünberg Institute (PGI-8), Forschungszentrum Jülich, 52425 Jülich, Germany*

1. Low-frequency noise properties

The noise spectra of Si NR structures were measured at the constant current in the ohmic CVC mode. Figure 6 shows the source-drain current low-frequency (LF) noise spectral density measured in dark conditions as well as under irradiation at back gate voltage of $V_{BG} = -1$ V and $I_{ds} = 0.1$ μA. Noise spectra, measured in dark, demonstrate $1/f^{\gamma}$ noise behavior with noise parameter equal to $\gamma = 1$. LF noise level rises with the increase of the light irradiation intensity. The increase of the illumination intensity results in the growth of the majority carrier's concentration. This in turn causes the growth of mobility fluctuations in the channel because of increased interaction and scattering rates as result of: first, scattering between carriers and secondly between the carriers and acoustic phonons, as well as on different impurity traps [20].

As the noise measurements were performed at the constant current in the ohmic CVC mode, the channel resistance linearly changes with the applied voltage V_{ds}. As it is known the $1/f$-noise spectral density is proportional to the voltage in power 2:

$$S_V = \frac{\alpha_H V_{ds}^2}{NR_{ch}^2 f^{\gamma}} = \frac{\alpha_H V_{ds}^2}{p\Omega R_{ch}^2 f^{\gamma}} = \frac{\alpha_H V_{ds}^2}{R_{ch}^2 f^{\gamma}} \frac{\alpha_H n^0}{Al} = \frac{\alpha_H V_{ds}^2}{f^{\gamma}} \frac{\alpha_H n}{l^2} \frac{1}{R_{ch}} \propto \frac{1}{R_{ch}}, \quad \frac{f^{\gamma} S_V}{V_{ds}^2} \propto \frac{1}{R_{ch}}. \tag{6}$$

Here R_{ch} is the current channel resistance; Ω, A and l is the volume, the cross-section area and the length of the current channel, respectively; μ_p is the majority carriers (holes) mobility and ρ is the channel specific resistance. The decrease of the channel resistance leads to growth of the noise spectral density. At the light excitation of NR FET sample with the special power W we have:

$$S_{V\perp} = \frac{\alpha_H V_{ds}^2}{NR_{ch}^2 f^{\gamma}} = \frac{\alpha_H V_{ds}^2}{p\Omega R_{ch}^2 f^{\gamma}} = \frac{\alpha_H V_{ds}^2}{\Omega f^{\gamma}} \frac{1}{p(\rho l/A)^2} = \frac{\alpha_H V_{ds}^2}{\Omega f^{\gamma}} \frac{A^2\sigma^2}{pl^2} = \frac{\alpha_H V_{ds}^2}{Alf^{\gamma}} \frac{A^2 e^2 p\mu_p^2}{l^2} =$$

$$= \frac{\alpha_H V_{ds}^2}{f^{\gamma}} \frac{A}{l^3} e^2 \mu_p^2 (p_d + \Delta p) = \frac{\alpha_H V_{ds}^2}{f^{\gamma}} \frac{A}{l^3} e^2 \mu_p^2 \left(p_d + \eta\alpha\tau_n \frac{W}{h\nu}\right). \tag{7}$$

Here p_d is the concentration of holes in the dark conditions, σ is the specific conductivity. The noise level increases proportionally to the intensity of the illumination.

We calculate values of the noise parameter γ, using the curves presented in Fig. 6. The following parameters are obtained for samples, measured in dark and at light excitation of different powers:

γ(dark) ≈1.0, γ(0.85 W/cm^2) ≈ 0.5 and γ(1.6 W/cm^2) ≈ 0.2.

Under irradiation the value of the noise parameter γ decreases. This can be explained as follows. With increasing light power, the conductivity of the current channel increases. As a result, the lifetime of minority carriers τ_n rises and reaches values $\tau_n \geq (10^{-2} \div 10^{-2})$ s. As is known, generation-recombination (g-r) noise has the Lorentzian shape

$$S_{V_{g-r}} \sim \frac{1}{1+(2\pi f\tau_n)^2}. \tag{8}$$

Here f is the frequency. It is clear that the section of the plateau on dependence $S_{V_{g-r}}(f)$ is determined by the condition

$$2\pi f_c \tau_n \leq 1. \tag{9}$$

It should be noted that with the increase in the lifetime of the electrons, first of all the value of the cut-off frequency f_c decreases. The characteristic frequency of the g-r noise shifts to the low-frequency region.

Since the conductivity σ and lifetime τ_n increase with increasing illumination power, the f_c decreases with increasing W, correspondingly:

$$f_c \propto \frac{1}{\tau_n} \propto \frac{1}{W}. \quad (10)$$

Secondly, the growth of g-r processes leads to an increase in the g-r noise level. These two processes result in the screening of the 1/f noise part under the g-r noise plateau. The fact explains the decrease in the value of the noise parameter γ with increasing illumination power. Note that the decrease in the value of the parameter γ can also be related to the growth of thermal noise due to the increase in the conductivity of the current channel.

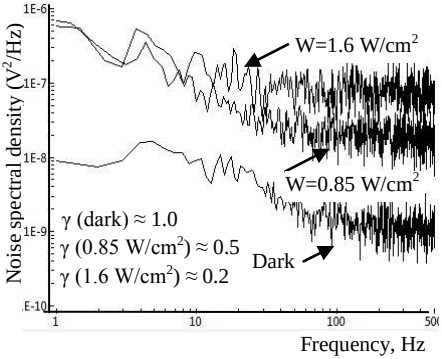

Fig. 6. Spectral dependence of LF noise, measured for NR FET sample with l = 10 μm under illuminations 0.85 W/cm^2; 1.6 W/cm^2, and in the dark, T=300K.

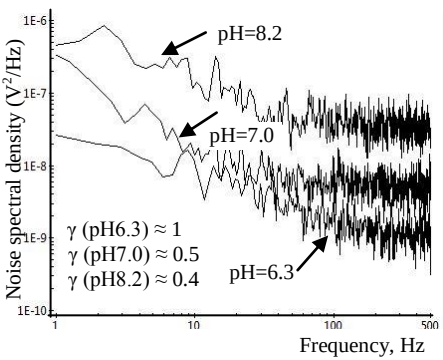

Fig. 7. Spectral dependence of LF noise for NR with length, l = 10 μm, measured at T= 300K and several pH values: 6.3, 7.0 and 8.2.

Figure 7 illustrates spectral dependency of the LF noise power spectrum of Si NR FET sample, measured at the $V_{FG} = -1$V, $I_{ds} = 0.1$ μA in solution at the several pH values: 6.3, 7.0 and 8.2. Noise parameter decreases with the increasing of the pH-value: γ(pH=6.3) ≈ 1.0; γ(pH=7.0) ≈ 0.5; γ(pH=8.2) ≈ 0.4. LF noise level increases and its slope decreases with increase of the pH-value. The increase in pH-value leads to a decrease in channel resistance, which is caused by the accumulation of negative charges at the semiconductor-oxide interface. Decreasing of the slope of $S_V(f)$ dependence can be explained taking into account the effect of the channel conductivity increasing.

2. Size-depending effects

In this section, we present the results of a study of the effect of SiNR characteristic length on the current transport mechanisms, pH-sensitivity, and also the behavior of LF noise. The magnitude of the current is inversely proportional to the length of the current channel, which justifies the application of the drift approximation for transport mechanism, as well as the assumption of a uniform distribution of the electric field strength along the length of the current channel (Fig. 8). The influence of light excitation, leads to an increase in the magnitude of the source-drain current. The pH-sensitivity increases with the current channel elongation and tends to the Nernst limit of 59.5 mV/pH, characteristic for micro-size sensors [19] (see Fig. 9). This behavior can be explained as follows. First, as the length of the channel l decreases, the area of the pH-sensitive surface decreases, and consequently the number of measurable H^+ ions in the aqueous solution decreases. Second, according to Eq.(2) the current I_{ds} increases with decreasing l, which leads to a decrease

in the resistance of the current channel at constant voltage V_{ds}. As the resistance of the channel R_{ch} decreases, its modulation is hampered under the influence of the H^+ ions; hence the pH- sensitivity decreases.

Figure 10 illustrates the LF noise spectral density dependencies on the length of the current channel. These curves are plotted using the spectral dependences of the LF noise measured in the dark conditions, under illumination with an intensity of 0.85 V/cm^2, and in an aqueous solution with a pH=7 of SiNRs of different lengths. Calculated value of the slope of those parallel curves is equal to $\log(500/10) \approx 2.7$ (see Fig. 10). This value is near the value (equal to 3) obtained theoretically using Eqns. (6) and (7), $S_V \propto l^{-3}$ with error about 10%. The difference between the theoretically expected and measured value of dependence $S_V(l)$ can be explained by relatively high level of thermal noise.

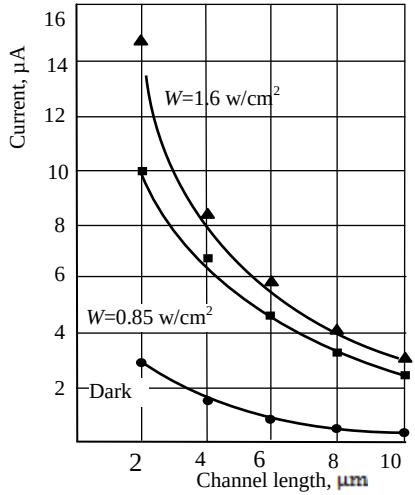

Fig. 8. Plot of channel current vs channel length. $V_{FG} = -10$ V, $V_{ds} = -5$ V, $R_{ch} = 1.26$ MΩ.

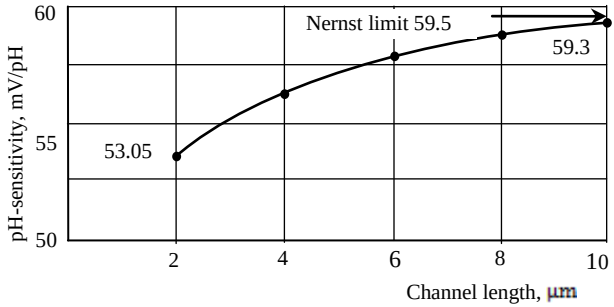

Fig. 9. Plot of pH-sensitivity vs channel length.
$V_{FG} = -10$ V, $V_{ds} = -5$ V, $R_{ch} = 1.26$ MΩ.

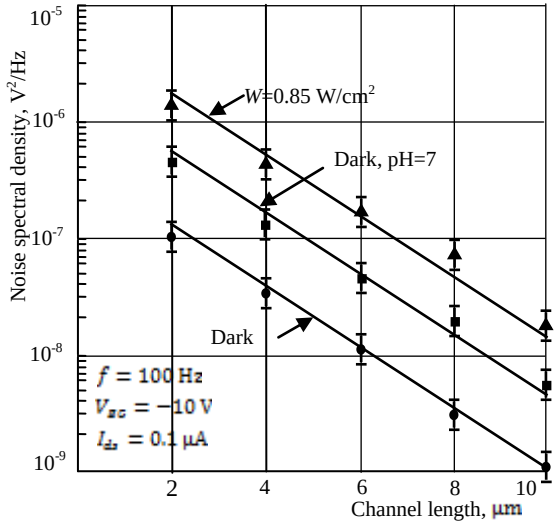

Fig. 10. Plot of noise spectral density vs channel length.

3. Conclusion

The spectral density of the LF noise increases both under the action of the pH solution and the illumination, and in both cases the frequency dependence of the noise is weakened and the value of the noise parameter γ decreases. With increasing of the pH and illumination power the 1/f noise is screened by the G-R plateau and the characteristic frequency of the G-R noise component decreases with increasing illumination power. LF noise level increases and its slope decreases with increase of the pH value. The magnitude of the channel current is approximately inversely proportional to the length of the current channel. The pH-sensitivity increases with the current channel elongation and approaches to the Nernst limit value of 59.5

mV/pH. It is shown that the measured value of the slope of noise spectral density dependence on the current channel length is 2.7 that are close to the theoretically predictable value 3.

Acknowledgments: This work was supported by the SCS MES of Armenia in the framework of research Project No. 15T-1C 279. F. Gasparyan greatly appreciates the support from the German Academic Exchange Service (DAAD) in the form of a research grant. The authors would like to acknowledge for the Innovation Award of RWTH Aachen University in the framework of RWTH transparent 2016.

References

1. ***R. Afrasiabi.*** Silicon Nanoribbon FET Sensors: Fabrication, Surface Modification and Microfluidic Integration. Doctoral thesis. Stockholm, Sweden 2016.
2. ***K.S. McKeating, A. Aubé, and J.-F. Masson.*** Analyst, **141**, 429 (2016).
3. ***H. Craighead.*** *Nature, **442**, 387 (2006).*
4. ***S.S. Bhinder, and P. Dadra.*** Asian J. of Chem., **21**, 5167 (2009).
5. ***G. Chen and L. Hu.*** SPIE Newsroom, 1087 (2008).
6. ***F. Gasparyan, H. Khondkaryan, A. Arakelyan, I. Zadorozhnyi, S. Pud, and S. Vitusevich.*** J. of Appl. Phys., **120,** 064902-(1-8) (2016).
7. ***L. Tsakalakos, J. Balch, J. Fronheiser, M.-Y. Shih, S. F. LeBoeuf, M. Pietrzykowski, P. J. Codella, B. A. Korevaar, O. Sulima, J. Rand, A. Davuluru, and U. Rapolc.*** J. Nanophotonics, **1**, 013552 (2007).
8. ***E. Garnett and P. Yang.*** Nano Lett., **10**, 1082 (2010).
9. ***V. Parkash and A. K. Kulkarni.*** IEEE Trans. Nanotechnol., **10**, 1293 (2011).
10. ***G. Sanders and Y.C. Chang.*** Phys. Rev., **B 45**, 9202 (1992).
11. ***A. Miranda, R.Vazquez, A. Dıaz-Mendez, and M. Cruz-Irisson.*** Microelectron. J., **40**, 456 (2009).
12. ***M. Bruno, M. Palummo, S. Ossicini, and R. D. Sole.*** Surf. Sci., **601**, 2707 (2007).
13. ***F.V. Gasparyan.*** Chapter 11: Noise Reduction in (Bio-) Chemical Sensors Functionalized with Carbon Nanotube Multilayers. Advanced Sensors for Safety and Security, NATO Science for Peace and Security Series B: Physics and Biophysics, A. Vaseashta and S. Khudaverdyan (eds.), DOI 10.1007/978-94-007 7003-4 11, © Springer ScienceCBusiness Media Dordrecht 2013, pp. 139-150.
14. ***S. Vitusevich, F. Gasparyan.*** Chapter 11: Low-Frequency Noise Spectroscopy at Nanoscale: Carbon Nanotube Materials and Devices. In: "Carbon Nanotubes Applications on Electron Devices" Ed. by J.M. Marulanda, PH InTech, 2011, pp. 257-296.
15. ***F.V. Gasparyan, A. Poghossian, S.A. Vitusevich, M.V. Petrychuk, V.A. Sydoruk, J.R. Jr. Siqueira, O.N. Oliveira, A. Offenhäusser, M.J. Schöning.*** IEEE Sensors Journal, **11**, 142 (2011).
16. *N. Elfström, A.E. Karlström and J. Linnros. Nano Lett.*, 8, 945 (2008).
17. ***T. Ytterdal, Y. Cheng and T. A. Fjeldly.*** Device Modeling for Analog and RF CMOS Circuit Design. John Wiley & Sons, Ltd, 2003.
18. ***F.V. Gasparyan, H.D. Khondkaryan.*** Proc. of the 10th Int. Conf. Semicond. Micro-and Nanoelectronics, Yerevan, Sept. 11-13, 2015, pp.68-71.
19. ***K. Bedner, V. A. Cuzenko, A. Tarasov, M. Wipf, R. L. Stoop, D. Just, S. Rigante, W. Fu, R. L. A. Minamisawa, Ch. David, M. Calame, J. Gobrecht, and Ch. Sch€onenberger.*** Sens. Mater, **25**, 567–576 (2013).
20. *S.V. Melkonyan, V.M. Aroutiounian, F.V. Gasparyan, H.V. Asriyan.* Physica, B: Physics of Condensed Matter, 382, 65 (2006).